Available online at www.sciencedirect.com

ScienceDirect

Energy Procedia 69 (2015) 1089 – 1099

Energy Procedia

International Conference on Concentrating Solar Power and Chemical Energy Systems
SolarPACES 2014

Thermoeconomic analysis of a solar dish micro gas-turbine combined-cycle power plant

L. Aichmayer[a], J. Spelling[b,*], B. Laumert[a]

[a] *Department of Energy Technology, KTH Royal Institute of Technology, 100 44 Stockholm, Sweden*
[b] *High Temperature Processes Unit, IMDEA Energy Institute, 28935 Móstoles, Spain*

Abstract

A novel solar power plant concept is presented, based on the use of a coupled network of hybrid solar-dish micro gas-turbines, driving a centralized heat recovery steam generator and steam-cycle, thereby seeking to combine the high efficiency of the solar dish collector with a combined-cycle power block. A 150 MW_e solar power plant was designed based on this concept and compared with both a conventional combined-cycle power plant and a hybrid solar-tower combined-cycle. The solar dish combined-cycle power plant could reach higher levels of solar integration than other concepts but was shown to be more expensive with current technology; solar electricity costs are double those of the hybrid solar-tower combined cycle.

Peer review by the scientific conference committee of SolarPACES 2014 under responsibility of PSE AG

Keywords: solar dish, micro gas-turbine, hybrid combined-cycle, solar hybridization, thermoeconomic analysis

1. Introduction

Concentrating solar power (CSP) is almost unique amongst renewable energy technologies in that it can supply controllable power on demand to consumers [1]. Through the integration of hybridization or thermal energy storage, CSP plants can continue generating power during cloud passages or at night, which makes them ideally suited to

* Corresponding author. Tel.: +34-91-737-1150; fax: +34-91-737-1140.
E-mail address: james.spelling@imdea.org

Peer review by the scientific conference committee of SolarPACES 2014 under responsibility of PSE AG
doi:10.1016/j.egypro.2015.03.217

form the backbone of a future low-carbon electricity grid, providing reliable generation capacity to support other renewable energy technologies.

However, despite these promising attributes, electricity from CSP plants remains more expensive than from solar photovoltaics and wind. As dispatchability is not currently valued by the majority of incentive schemes [2], CSP plants cannot exploit their unique characteristics and deployment has slowed in recent years. Central to the challenges faced by CSP is the fact that over 80% of all installed capacity is still based on low temperature parabolic trough technology [3], developed nearly 30 years ago. More recent central receiver systems operate at higher temperatures; however, electricity costs are still high, making investments highly dependent on subsidies. In order to achieve significant cost reductions, a step change in CSP technology is needed.

Increasing the efficiency of CSP plants is seen as key to reducing electricity costs, as this will contribute to reduce the size of the solar field, which is the most expensive component of the power plant. As such, the highest efficiency solar collector technology should be combined with the highest efficiency thermal power block, and one option, first proposed by Karni [4], is to employ parabolic dish concentrators combined with a combined-cycle power block, to give a solar dish combined cycle power plant.

2. Solar dish power generation systems

Solar dish systems are currently the solar power technology that has demonstrated the highest conversion efficiency [5]. However, due to optical constraints, the size of a single dish is limited, with typical thermal outputs in the region of 45 to 75 kW_{th} [6]. As such, they are commonly used for distributed power generation, combined with either Stirling engines or micro-turbine power blocks, with electrical outputs between 15 and 25 kW_e per unit [6]. The ability to hybridize the power block with diesel, or locally-produced biofuels, increases the reliability and availability of dish systems compared to stand-alone photovoltaic installations, and reduces costs when compared with expensive battery storage [7]. Small-scale solar polygeneration systems have been studied in detail by the authors [8], and have been shown to be economically attractive for off-grid applications.

When moving towards utility-scale applications, the standard approach has been to simply combine a large number of solar dish units at a single location to form a dish farm with the desired capacity. However, the size of the individual solar collectors and power conversion units remains small, leading to high specific costs. As such, despite the high efficiency of solar dish systems, their cost of electricity remains higher than central receiver or parabolic trough power plants, which are able to harness the economies of scale associated with larger solar fields and power blocks to reduce electricity costs, despite their lower conversion efficiencies.

2.1. The solar dish micro gas-turbine combined cycle power plant

The solar dish micro gas-turbine combined cycle (MGTCC) is an alternative to conventional solar dish farms, which seeks to combine the high efficiency of the solar dish collector with economies of scale from the use of large combined-cycle power blocks. The power plant consists of an array of hybrid solar dish micro gas-turbines (MGTs) from which the exhaust gases are collected and used to drive a single large steam-cycle, giving a utility-scale CSP plant. Hybrid operation is an attractive feature of the MGTCC, facilitating control and ensuring the availability of the power plant to meet demand whenever it occurs. Guaranteed electricity production (by supplementing solar heat with fuel when the irradiation is insufficient) reduces the economic risks associated with such plants.

A typical layout of an MGTCC power plant is shown schematically in Fig. 1. A piping network is used to collect the exhaust gases from the array of hybrid solar MGTs and deliver them to a conventional heat recovery steam generator and dual-pressure steam-cycle; to minimize water consumption the steam-cycle is dry-cooled.

Contemporary metallic-rotor MGTs are designed with combustor outlet temperatures in the region of 900°C [10], a good match with the current generation of volumetric solar receivers which can operate with outlet temperatures up to 1000°C [11]. The MGTCC power plant can therefore be operated using up to 100% solar energy when irradiation conditions are favorable. As both the receiver and MGT are mounted at the focal spot of the solar dish collector the two can be closely integrated, simplifying operation and increasing efficiency. The close integration of the receiver and combustion chamber of the MGT also eliminates the temperatures limitations due to hot-gas piping that are

encountered in larger hybrid gas-turbine systems (where the solar receiver must be mounted at the top of the central tower); this allows the full potential of high-temperature volumetric receivers [12] to be exploited by the MGTCC.

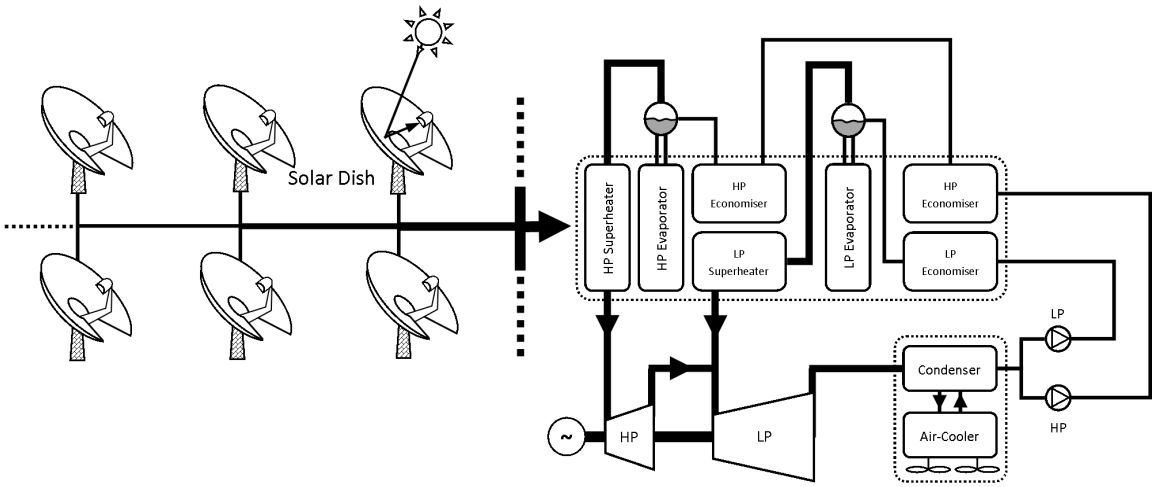

Fig. 1. Schematic layout of a solar dish micro gas-turbine combined cycle power plant.

3. Thermoeconomic modeling of the solar dish micro gas-turbine combined cycle power plant

In order to analyze the performance of the MGTCC, a 150 MW_e power plant has been designed and evaluated using the in-house thermoeconomics tool: DYESOPT (for DYnamic Energy Systems OPTimiser), which is described in detail in previous works [8] [13]. The novel power plant is compared with both an equivalent unmodified utility-scale combined-cycle power plant, as well as a hybrid solar tower combined-cycle (HSTCC) power plant based on a single large hybrid gas-turbine coupled with heliostat field solar collector technology. In a previous study by the authors [13], the HSTCC power plant was shown to be the most economically attractive of the hybrid solar combined cycles configuration studied to date.

3.1. Nominal power block design

Integration of solar heat into a hybrid MGT can be done in many ways, as explored previously by the authors [9]. While internally-fired recuperated MGTs were shown to be the most cost-effective in stand-alone applications, their exhaust temperature is too low for combined-cycle applications (in the region of 150°C). As such, an open-cycle MGT is used in the MGTCC, as shown in Fig. 2. In order to achieve an exhaust temperature of 540°C, typical for F-class combined cycles [14], an open-cycle MGT with a combustor outlet temperature of 900°C needs to operate with a pressure ratio of 5.1:1. The open-cycle MGT also has the advantage of a significantly reduced weight (due to the removal of the recuperator), which will facilitate integration with the dish, as well as reducing costs [10].

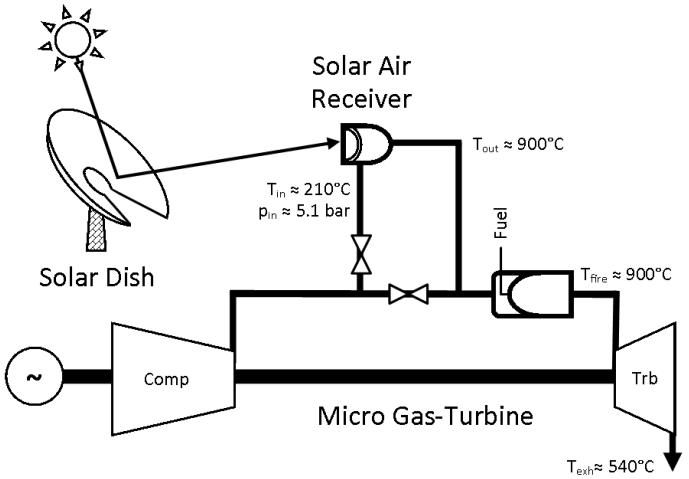

Fig. 2. Open-cycle hybrid solar-dish micro gas-turbine.

The procedure used to establish the nominal sizing of the MGTCC power block is different than would be expected for a conventional combined-cycle power plant [14], where the gas-turbine and steam-cycles are simply matched and then sized to the meet the desired power output. In the case of the MGTCC a significant additional constraint is imposed by the maximum size (and thus collector area) of each individual dish unit, which limits the maximum solar heat input to the MGT. As such, if a given fraction f_{sol} of the total nominal heat input to the MGT is to be supplied by the solar dish, the size of the MGT unit is given by Equation (1), as a function of the dish aperture A_{dish}, the optical efficiency of the dish η_{opt}, the thermal efficiency of the receiver η_{rec}, the conversion efficiency of the MGT η_{MGT} and the reference solar beam radiation I_b at design conditions. The maximum size of the MGT is limited by the weight that can be mounted at the focus spot of the dish; a limit of 150 $\mathrm{kW_e}$ has been considered here.

$$\dot{E}_{\mathrm{MGT}}^{nom} = \frac{A_{dish}\eta_{opt}\eta_{rec}^{nom}\eta_{\mathrm{MGT}}^{nom}I_b^{ref}}{f_{sol}^{nom}} \tag{1}$$

Once the size of each individual MGT has been determined, the required number of dishes N_{dish} in the MGTCC array can be calculated using Equation (2), where E_{MGTCC} is the desired nominal output of the power plant, η_{SC} is the conversion efficiency of the bottoming steam-cycle and η_{pipe} is the thermal efficiency of the piping network that delivers the exhaust gases from the MGT array to the central steam-cycle (see §3.3).

$$N_{dish} = \frac{\dot{E}_{\mathrm{MGTCC}}^{nom}}{\dot{E}_{\mathrm{MGT}}^{nom}\cdot\left(1+\eta_{pipe}\cdot\frac{\left(1-\eta_{\mathrm{MGT}}^{nom}\right)}{\eta_{\mathrm{MGT}}^{nom}}\eta_{\mathrm{SC}}^{nom}\right)} \tag{2}$$

3.2. Off-design power plant performance

The off-design models of the topping gas-turbine and bottoming steam-cycle are based on the fixed and variable heat rate model [15], which distinguishes between the fixed heat that is required to drive the turbines at full speed and maintain synchronization with the grid (at zero output) and the variable heat that is required to produce power. As can be seen in Fig. 3, this model effectively captures the efficiency penalty for operating the power cycles at part-load conditions. In numerical terms, the heat rate model can be expressed using Equation (3), where Q is the heat input required to produce a given electrical output E, and E_{nom} is the nominal output of the power unit.

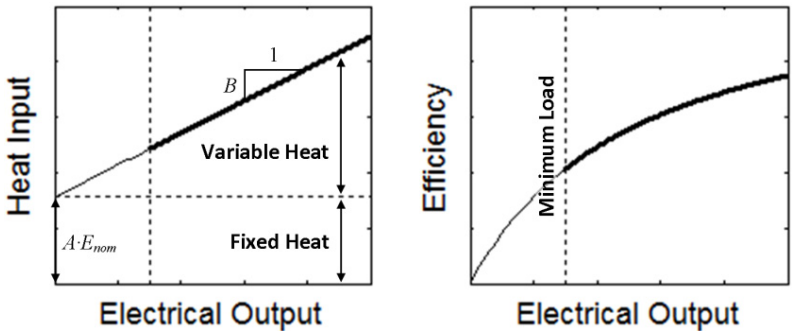

Fig. 3. Fixed and variable heat rate model for thermal power cycle modeling.

The constants A and B are determined using Equation (4), based on the efficiency of the power cycle at full load η_{nom} and at 50 % load η_{50}. Equation (3) is used to model both the topping gas-turbine and bottoming steam-cycle, with different values of the constants A and B, based on the relevant efficiencies.

$$\dot{Q} = A \cdot \dot{E}_{nom} + B \cdot \dot{E} \tag{3}$$

$$A = \frac{1}{\eta_{50}} - \frac{1}{\eta_{nom}} \quad \text{and} \quad B = \frac{2}{\eta_{nom}} - \frac{1}{\eta_{50}} \tag{4}$$

In a hybrid MGTCC power plant more than one heat source is present, as solar heat is combined with fuel input to drive the MGT, and the basic heat rate model needs to be modified to take this into account, giving Equation (5). The heat input Q_{SC} for the bottoming steam-cycle is derived from the MGT exhaust; applying the conservation of energy to Equation (3), the exhaust heat Q_{SC} delivered to the steam-cycle can be determined using Equation (6).

$$\dot{E}_{\mathrm{MGT}} = \frac{\left(\dot{Q}_{fuel} + \dot{Q}_{sol}\right) - A_{\mathrm{MGT}} \cdot \dot{E}_{\mathrm{MGT}}^{nom}}{B_{\mathrm{MGT}}} \tag{5}$$

$$\dot{Q}_{\mathrm{SC}} = \eta_{pipe} \cdot \left(A_{\mathrm{MGT}} \cdot \dot{E}_{MGT}^{nom} + \left(B_{\mathrm{MGT}} - 1\right) \cdot \dot{E}_{\mathrm{MGT}}\right) \tag{6}$$

The solar heat input to the MGT can be calculated using Equation (7) as a function of the beam radiation I_b and the variable thermal efficiency η_{rec} of the receiver, which can be estimated directly from the current beam radiation intensity using a simple constant surface temperature model.

$$\dot{Q}_{sol} = A_{dish} \eta_{opt} \eta_{rec} I_b \quad \text{where} \quad \eta_{rec} = 1 - \left(1 - n_{rec}^{nom}\right) \cdot \frac{I_b^{ref}}{I_b} \tag{7}$$

Using the different the heat rate models presented above, the fuel input to the MGTCC can be determined as a function of the required load and the varying solar heat input. This fuel consumption can then be directly linked to the fuel costs and the environmental impact of the power plant.

3.3. Dish-piping network design

The dish-piping network collects the exhaust gases from each individual MGT unit and delivers them to the heat recovery steam generator and steam-cycle. The dish network is based on a tree-and-branch structure, as shown in Fig. 4, where the dish field is divided into a number of segments, each of which has a main pipe running out perpendicular to the central steam-cycle power block. Individual dishes are placed along this pipe with a given spacing l_{sp}, and at each dish location the pipe branches out at 90°, along which additional dishes are placed with the

same spacing, until they approach too close to the segment boundary. Within this matrix of possible locations, dishes are placed to minimize the total piping distance, in order to keep both thermal and pressure losses to a minimum.

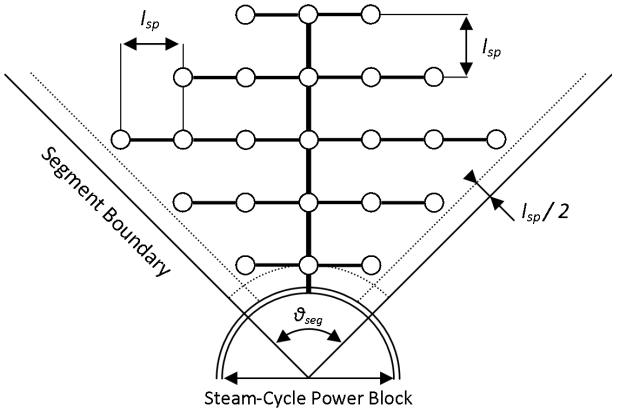

Fig. 4. Schematic layout of the dish-piping network.

Once the locations of the dishes are determined and the piping network layout is fixed, the thermal efficiency of the piping network can be determined. The network is modeled as a series of heat exchangers where the atmosphere is treated as a heat sink with an infinite heat capacity rate. Heat transfer from the exhaust gas to the atmosphere takes into account the forced convention within the gas, conduction through the piping insulation and natural convection of heat out to the air; mineral wool was assumed for the insulating material. Thermal losses act to reduce the heat available to the bottoming steam-cycle, decreasing the overall conversion efficiency of the power plant.

Pressure losses have also been calculated, using a standard hydraulic network approach with the Darcy-Weisbach equation used to calculate the head loss [16]; additional mixing pressure losses were considered at each pipe intersection. Pressure losses increase the back-pressure to the MGTs, which results in an efficiency penalty.

3.4. Equipment cost functions and electricity costs

The total construction cost C_0 for the hybrid MGTCC power plant takes into account the cost of the power block (including the MGT units, the integrated solar receivers, the piping network and the bottoming steam-cycle) the cost of the solar dish equipment, the cost of equipment installation, the costs associated with engineering and procurement as well as contingency costs.

An overview of the capital costs for the power plant components is given in Table 1. Costs for the simple-cycle MGT unit are taken from Bowman Power Systems [17], and are lower than for conventional domestic MGTs due to the removal of the recuperator, which represents a significant fraction of the total cost [10]. Costs for the solar dish collectors and the pressurized air receiver are taken from SolarPACES figures [18], while costs for the bottoming steam-cycle are taken from the Gas Turbine World handbook [19]. Costs for the piping network are taken from Nordman [20]. Installation costs were assumed to be 15% of the capital costs [21] and the costs of engineering and procurement to be 5% of the installed cost [22]; contingency costs were estimated as 10% of the installed cost [23].

Table 1. Capital and maintenance costs for the power plant components.

Power Plant Component	**Capital Cost**	**Fixed O&M**	**Variable O&M**
Solar Dish Collectors	425 USD/m^2	2.33 USD/m^2yr	-
Pressurized Air Receiver	185 USD/kW_{th}	11.0 USD/kW_{th}yr	0.69 USD/MWh_{th}
Micro Gas-Turbine (80 kW_e)	962 USD/kW_e	24.9 USD/kW_eyr	1.49 USD/MWh_e
Gas Piping Network	520 USD/m	2.86 USD/m·yr	-
Bottoming Steam Cycle	1478 USD/kW_e	28.3 USD/kW_eyr	0.96 USD/MWh_e

The costs for the MGT are based on an 80 kW_e unit; however, the size of the MGT can vary considerably as the solar share is changed. Smaller units will increase the specific costs, resulting in proportionally more expensive units. The total cost of the MGT unit can be scaled using Equation (8) to take this into account.

$$C_{\mathrm{MGT}} = C_{\mathrm{MGT}}^{80\mathrm{kW}} \cdot \left(\frac{\dot{E}_{MGT}^{nom}}{80\mathrm{kW}} \right)^{0.7} \tag{8}$$

The annual maintenance costs of the power plant C_{mnt}, includes both fixed and variable costs as well as cycling costs, which result from the start-up and shutdown of the power block. An overview of the fixed and variable maintenance costs for the different power plant components is also given Table 1. Maintenance costs were obtained from the same sources as the capital costs, with the split between fixed and variable costs calculated based on the work of Johnson [24]. The solar dishes and piping are exposed to the weather, and thus require maintenance regardless of use; no variable costs are associated with these components. Maintenance costs due to cycling can be determined using the equivalent operating hours approach [25].

The levelized cost of electricity (LCOE) can be calculated using Equation (9), where C_{fuel} is the annual fuel cost and E_{net} is the net annual electricity production. The annuity factor α is calculated based on the interest rate i and the power plant operating lifetime n_{op}. Standard values for these financing parameters can be obtained from the ECOSTAR report [18], giving $\alpha = 9.88\%$.

$$\mathrm{LCOE} = \frac{\alpha \cdot C_0 + C_{mnt} + C_{fuel}}{E_{net}} \qquad \text{where} \qquad \alpha = \frac{i \cdot (1+i)^{n_{op}}}{(1+i)^{n_{op}} - 1} \tag{9}$$

Of further interest is the levelized cost of the solar-derived electricity (LCOE_{sol}), determined using Equation (10) based on the price at which the solar electricity must be sold in order to be able to sell the fossil-derived share of the electricity at the same price (LCOE_{ref}) as the unmodified CCGT power plant; the annual value of f_{sol} is used.

$$\mathrm{LCOE}_{\mathrm{sol}} = \frac{\mathrm{LCOE} - (1 - f_{sol}) \cdot \mathrm{LCOE}_{\mathrm{ref}}}{f_{sol}} \tag{10}$$

4. Thermoeconomic analysis

Having established a thermoeconomic model of the hybrid MGTCC power plant, this model can now be used to analyze the performance of the system. The power plant is designed for a nominal output of 150 MW_e, and the performance of the individual power plant components is summarized in Table 2. The performance of the reference combined-cycle and HSTCC power plants can be calculated using the models established in a previous work [13].

The performance of the MGTCC power plant depends on a number of meteorological and economic boundary conditions. The power plant is assumed to be located in Kuraymat, Egypt, at 29.2°N, with an annual direct normal insolation of 2431 kWh/m^2yr [26]; radiation data was taken from the HelioClim3 service [27]. A price of 25.1 USD/MWh_{th} was assumed for natural gas, which was taken to be an 85-10-5 mixture of methane, ethane and propane, giving a lower heating value of 49.6 MJ/kg and a carbon content of 75.8% by weight. The power plants are assumed to be operated at full load between 7 am and 11 pm, regardless of the solar irradiation conditions.

Table 2. Power plant component efficiencies.

Nominal Component Efficiencies		
Micro Gas-Turbine	15	[%]
Bottoming Steam-Cycle	31	[%]
Pressurized Air Receiver	78	[%]
Solar Dish Collector	87	[%]

Having fixed the system specifications and boundary conditions, the design parameters can be chosen. In this work, focus is placed the sizing of the solar equipment and, as such, the main design parameter for the MGTCC concerns selection of the nominal solar share of the MGT unit. This will influence the sizing of the MGT units and the operating temperature of the receiver; a maximum temperature of 900°C is considered, allowing 100% solar operation when conditions are favorable. For the HSTCC power plant, a nominal receiver temperature of 800°C is considered due to piping constraints, giving a nominal solar share of 33.7%; only the heliostat field size is varied.

4.1. Thermoeconomic performance of the solar dish micro gas-turbine combined cycle power plant

The first performance factor considered is the economic viability of the power plant. The specific costs of the MGTCC and HSTCC power plants are shown in Fig. 5, and the behavior of the two systems is very different. Unlike the HSTCC configuration, where there is a fixed power block cost increase for hybridization of the topping gas-turbine (due receiver integration and construction of the central tower and piping), the specific cost of the MGTCC power block increases as the annual solar share increases. As can be seen in Fig. 6, this is due to the fact that as the solar share increases, the size of the MGT units decreases, due to the limited solar heat input that can be provided by a single dish (see §3.1); this results in an increase in the specific cost of the MGT. The number of dishes also rises with increasing solar shares, leading to an increase in piping and solar collector costs.

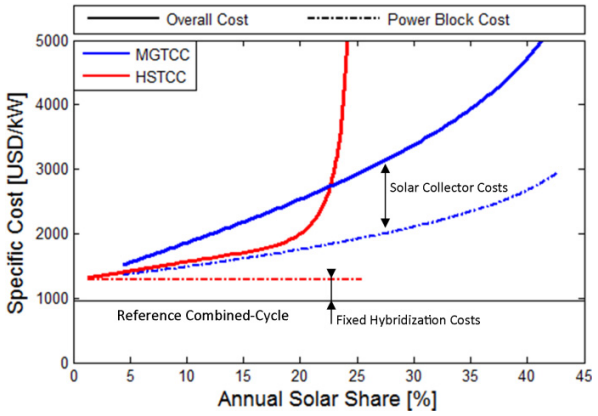

Fig. 5. Hybrid power plant specific costs.

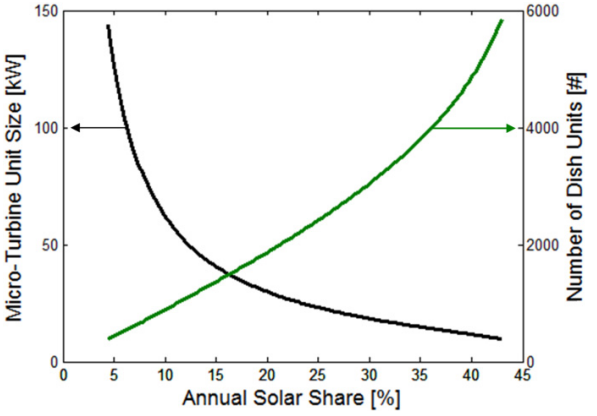

Fig. 6. Micro gas-turbine unit sizing and numbers.

The influence of solar integration on the cost of electricity is shown in Fig. 7, both in terms of the overall LCOE (solid line) and the LCOE of the solar-derived electricity (dashed-line). It can be seen that while the MGTCC power plant reaches higher solar shares than the HSTCC, with a maximum of 42.7% for the MGTCC compared to 25.5% for the HSTCC, its electricity costs are significantly higher. At low-to-moderate annual solar shares, the overall LCOE of the HSTCC is only 12.2% higher than the unmodified combined-cycle power plant, compared to 63.4% for the MGTCC. When examining the solar LCOE, it can be seen that while the optimal MGTCC configuration provides a 12.5% reduction in costs compared to a pure-solar dish MGT system (using a recuperated MGT), solar electricity costs are still 46.1% higher than from a contemporary molten-salt tower CSP plant [22], making the MGTCC configuration uncompetitive. The optimal HSTCC configuration, on the other hand, offers a 26.8% reduction in solar electricity costs compared to the molten-salt tower CSP plant.

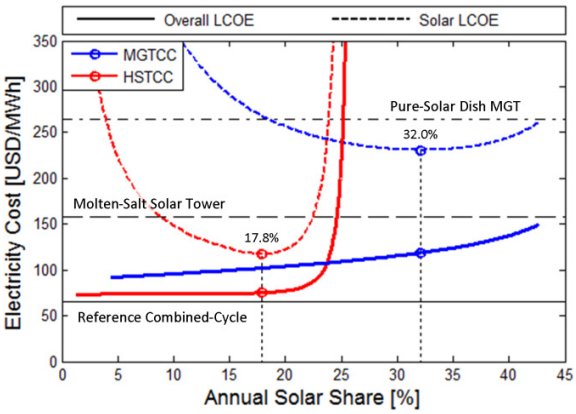

Fig. 7. Hybrid power plant specific costs.

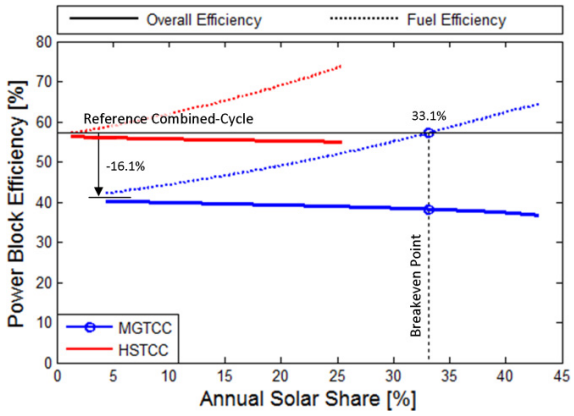

Fig. 8. Hybrid power plant efficiencies.

A significant factor in the poor economic performance of the MGTCC power plant is the lower power block efficiency of this configuration. The low efficiency of the topping MGT (15%, compared to ~38% for a typical combined-cycle gas-turbine) shifts power production to the bottoming-cycle, resulting in a 16.1%-point penalty to the power-block efficiency. As a result of this lower fuel conversion efficiency, the solar fraction of electricity must be sold at a high price in order for the fuel-derived electricity to be competitive with the reference combined-cycle.

This poor conversion efficiency also harms the environmental performance of the power plant. As shown in Fig. 8, the MGTCC must operate with an annual solar share of at least 33.1% in order to simply reach the same fuel efficiency as an unmodified combined-cycle power plant, whereas the HSTCC can effectively harness the solar energy to reach fuel-efficiencies in the region of 74%, offering significant reductions in power plant emissions.

4.2. Optimal power plant designs

Using the solar LCOE, optimal power plant configurations can be identified for both the MGTCC and HSTCC configurations, and are compared against the reference combined-cycle power plant in Table 3. The lower power block efficiency of the MGTCC can clearly be seen, along with the shift of power capacity to the bottoming steam-cycle. Emissions from the optimal MGTCC are actually 1.7% higher than from an unmodified combined-cycle power plant, making the MGTCC configuration unattractive from both economic and environmental standpoints.

Table 3. Comparative performance of the optimal power plant designs.

Power Plant Performance	**Reference CCGT**	**MGTCC**	**HSTCC**	
Nominal Power Output	150	150	150	[MWe]
Power Block Efficiency	57.2	38.2	55.4	[%]
Gas-Turbine Capacity	99.6	56.2	100.5	[MWe]
Steam-Cycle Capacity	50.4	105.6	56.3	[MWe]
Nominal Solar Share	-	66.4	33.7	[%]
Annual Solar Share	-	32.0	17.8	[%]
Overall Electricity Cost	65.8	118	74.7	[USD/MWh$_e$]
Solar Electricity Cost	-	231	116	[USD/MWh$_e$]
Specific CO_2 Emissions	402	409	341	[kg$_{CO2}$/MWh$_e$]

5. Conclusions

A detailed techno-economic analysis has been performed for a novel 150 MW_e hybrid solar dish micro gas-turbine combined-cycle power plant, based on the use of a coupled network of hybrid solar-dish micro gas-turbines, driving a centralized heat recovery steam generator and steam-cycle, thereby seeking to combine the high efficiency of the solar dish collector with a high-efficiency and low-cost combined-cycle power block.

With the system specifications considered in this work, the higher specific cost of the micro gas-turbine units and the lower power block efficiency of the novel cycle concept result in increases in both the upfront capital costs and the levelized electricity costs. The optimal design has a predicted solar electricity cost of 231 USD/MWh_e, 46.1% higher than from a contemporary molten-salt tower CSP plant. At the same time, emissions are 1.7% higher than from a standard unmodified combined-cycle power plant, making the micro gas-turbine combined-cycle appear to be both economically and environmentally unattractive with current technology.

A key challenge when drawing conclusions from this work lies in the fact that both the hybrid solar combined-cycle concepts analyzed are currently prototype systems, and considerable effort is needed to bring them to maturity. Significant cost reductions have been observed for central receiver systems in recent years as deployment has accelerated, and it is likely that mass production would yield similar costs reductions for solar dish systems. Furthermore, advances in solar micro-turbine technology, such as closer receiver integration, will increase power block performance and bring down costs, allowing the true potential of hybrid solar dish micro gas-turbine combined-cycle power plants to be unlocked, especially in high solar-share configurations.

As such, in addition to being ideally suited for small-scale stand-alone and off-grid applications, hybrid solar dish micro gas-turbines also have great potential for utility-scale power production. Future studies will seek to further refine and optimize the design of these hybrid systems and identify the most efficient and cost-effective solutions.

Acknowledgements

This work has been co-funded by the European Commission as part of the FP7 Optimised Microturbine Solar Power System project (OMSoP - grant agreement 308952), the support of which is gratefully acknowledged.

References

[1] International Energy Agency, 2011, *Renewable Energy Technologies: Solar Energy Perspectives*, OECD/IEA Publications, Paris

[2] J. Sawin, R. Adib, J. Skeen et al., 2013, *Renewables 2013 - Global Status Report*, Renewable Energy Policy Network, United Nations Environment Programme, Paris

[3] A. Fernández-García, E. Zarza, L. Valenzuela et al., *Parabolic-Trough Solar Collectors and their Applications*, Renewable and Sustainable Energy Reviews, Volume 14/7 (2010), pp. 1695 – 721

[4] J. Karni, 2013, *Keynote Speech*, International SolarPACES Conference, September 17 – 20, Las Vegas

[5] M. Romero, J. González-Aguilar, *Solar Thermal CSP Technology*, WIREs Energy and Environment, Volume 3 (2014), pp. 42 – 59

[6] V. Siva Reddy, S. Kaushik, K. Ranjan et al., *State-of-the-Art Solar Thermal Power Plants – A Review*, Renewable and Sustainable Energy Reviews, Volume 27 (2013), pp. 258 – 73

[7] R. Buck, S. Friedmann, *Solar-Assisted Small Solar Tower Trigeneration Systems*, Journal of Solar Energy Engineering, Volume 129/11 (2007); pp. 349 – 54

[8] L. Aichmayer, J. Spelling, B. Laumert, 2013, *Small Scale Hybrid Solar Power Plants for Polygeneration in Rural Areas*, Proceedings of the ISES Solar World Congress, November 3 – 7, Cancun

[9] L. Aichmayer, J. Spelling, B. Laumert et al., *Micro Gas-Turbine Design for Small-Scale Hybrid Solar Power Plants*, Journal of Engineering for Gas Turbines and Power, Volume 135/11 (2013)

[10] A. Malmquist, 2012, *Personal Communication*, COMPOWER AB, Lund

[11] P. Heller, M. Pfänder, T. Denk et al., *Test and Evaluation of a Solar Powered Gas Turbine System*, Solar Energy, Volume 80 (2006), pp. 1225 – 230

[12] A. Avila-Marin, *Volumetric Receivers in Solar Thermal Power Plants with Central Receiver System Technology: A Review*, Solar Energy, Volume 85 (2011), pp. 891 – 910

[13] J. Spelling, B. Laumert, 2014, *Thermoeconomic Evaluation of Solar Thermal and Photovoltaic Hybridization Options for Combined-Cycle Power Plants*, GT2014-25173, Proceedings of the ASME Turbo Expo, June 16 – 20, Düsseldorf

[14] R. Kehlhofer, F. Hannemann, F. Stirnimann et al., 2009, *Combined-Cycle Gas and Steam Turbine Power Plants*, Third Edition, PennWell Corporation, Tulsa

[15] C. Harris, 2006, *Electricity Markets – Pricing, Structures and Economics*, John Wiley & Sons, Chichester

[16] F. Incropera, D. De Witt, T. Bergman et al., 2007, *Fundamentals of Heat and Mass Transfer*, Sixth Edition, John Wiley & Sons, New York
[17] K. Mehrayin, 2002, *Microturbines and their use in Small Scale Cogeneration*, Bowman Power Systems, Southampton
[18] R. Pitz-Paal, J. Dersch, B. Milow et al. (editors), 2004, ECOSTAR: European Concentrated Solar Thermal Road-Mapping
[19] Gas Turbine World, 2012, *Gas Turbine World Handbook: Project Planning, Pricing, Engineering, Construction and Operation*, Pequot Publishing Inc., Fairfield
[20] R. Nordman, 2005, *New Process Integration Methods for Heat-Saving Retrofit Projects in Industrial Systems*, PhD Thesis, Chalmers University of Technology, Gothenburg
[21] M. Peters, K. Timmerhaus, 1991, *Plant Design and Economics for Chemical Engineers*, Fourth Edition, McGraw-Hill, New York
[22] C. Turchi, G. Heath, 2013, *Molten Salt Power Tower Cost Model for the System Advisor Model*, National Renewable Energy Laboratory, (NREL/TP-5500-57625)
[23] International Energy Agency, 2010, *Projected Cost of Generating electricity*, OECD/IEA Publications, Paris
[24] B. Johnson, 2008, *Better Model Inputs: Estimating Fixed and Variable O&M Costs*, White Paper, University of Chicago, retrieved from press.ci.uchicago.edu
[25] International Organization for Standardization, 1999, *Gas Turbines – Procurement -- Part 9: Reliability, Availability, Maintainability and Safety*, ISO 3977-9:1999, Geneva
[26] G. Brakmann, K. Fekry, A. Fayek, 2006, *ISCC Kuraymat - Integrated Solar Combined Cycle Power Plant in Egypt*, Proceedings of the International SolarPACES Conference, June 20 – 23, Seville
[27] SoDa Solar Radiation Data, 2013, *Time Series of Solar Radiation Data*, retrieved from www.soda-is.com